Appendix G Aerodynamic Data of Real Aircraft

- Subsonic & Supersonic Drag Polars
- C_{D_0} & $C_{D_{min}}$ vs Mach Number
- Maximum L/D Correlation Curve
- Subsonic C_{D_0} Correlation Curve
- Wing Efficiency Factor Correlation
- Boeing/DARPA Condor ISR Aircraft

Cessna 172 Skyhawk, a four-seat, single-engine, high-wing, unpressurized general aviation aircraft. First flown in 1955, it is still in production. Over 43,000 have been built, more than any other aircraft. The number of variants have been relatively few, a testament to the original design. A case study appears in Volume II.

Few things are created and perfected at the same time.

G.1 How To Use Aerodynamic Data

This appendix contains aerodynamic data on real aircraft. There is drag polar data on propeller aircraft, turbine transports and military cargo aircraft, fighter aircraft, and intelligence, surveillance, and reconnaissance (ISR) aircraft (Figs. G.1–G.9). All aero coefficients are referenced to the aircraft reference area (S_{ref}), which is the total planform wing area. These data are to be used by the designer as a starting point for initial sizing and then as a sanity check on the aero estimates.

When using these data the designer must understand the mission of the aircraft because the mission drives the configuration, which drives the resulting aerodynamics. When designing an apple, use the data from other apples. It is interesting to observe that the aero data for wing–body–tail

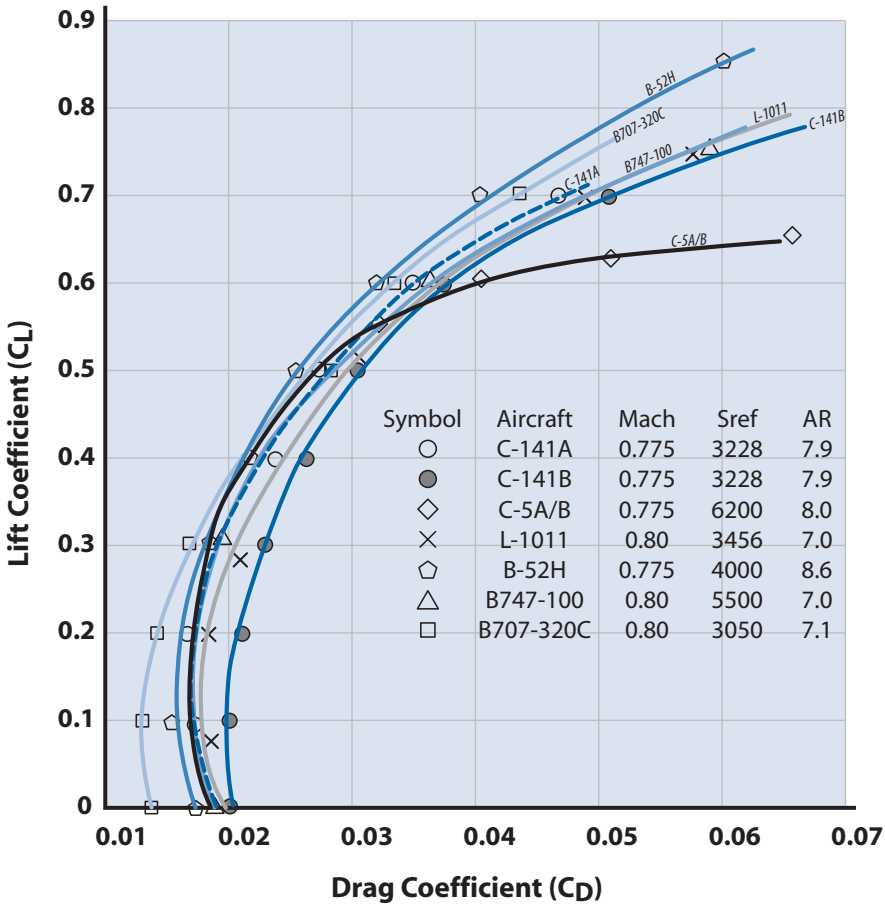

Figure G.1 High-subsonic drag polars for large transport aircraft—flight test data.

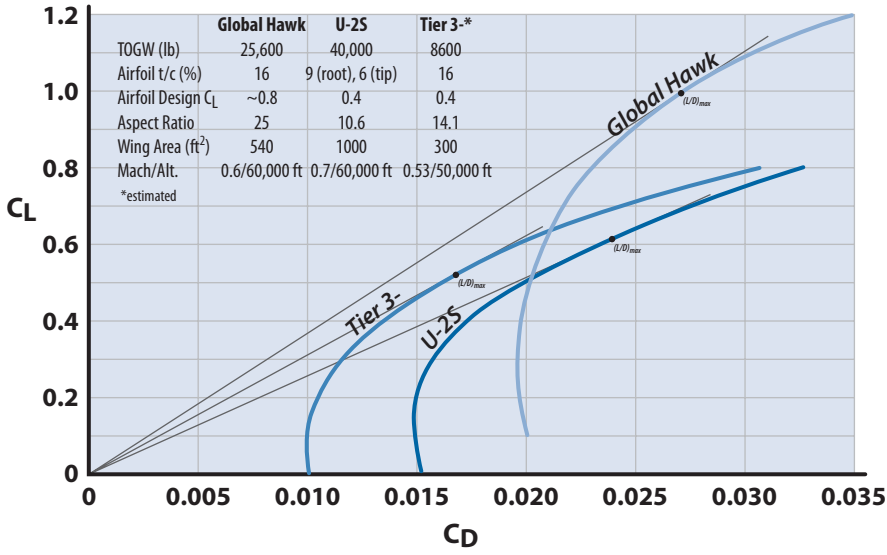

Figure G.2 Drag polars for ISR aircraft.

transport and fighter configurations collapse into a relatively tight band for the subsonic drag polars (see Figs. G.1, G.4, and G.6) and $C_{D_{\min}}$ vs Mach number (see Fig. G.5). However the $C_{D_{\min}}$ data for swept-wing tailless configurations fall well outside this band (see the F-106 and B-70 in Fig. G.5).

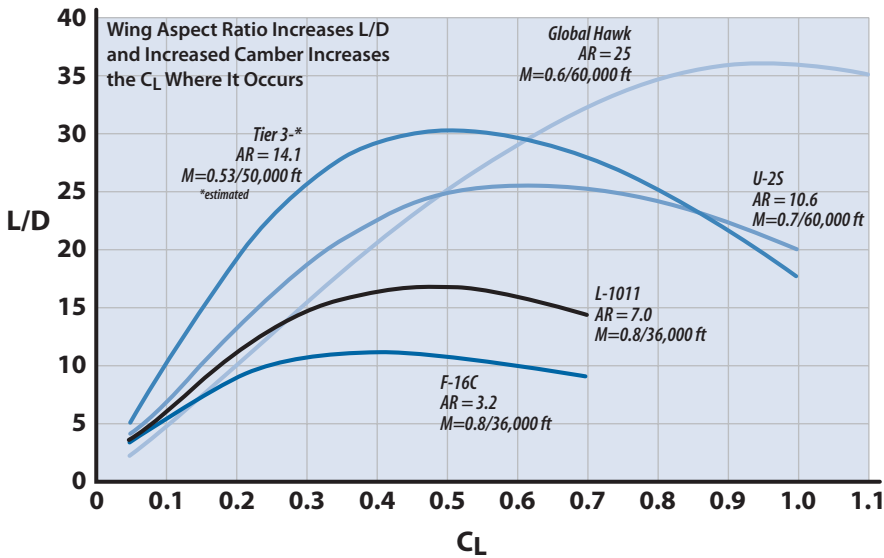

Figure G.3 L/D vs C_L for various aircraft.

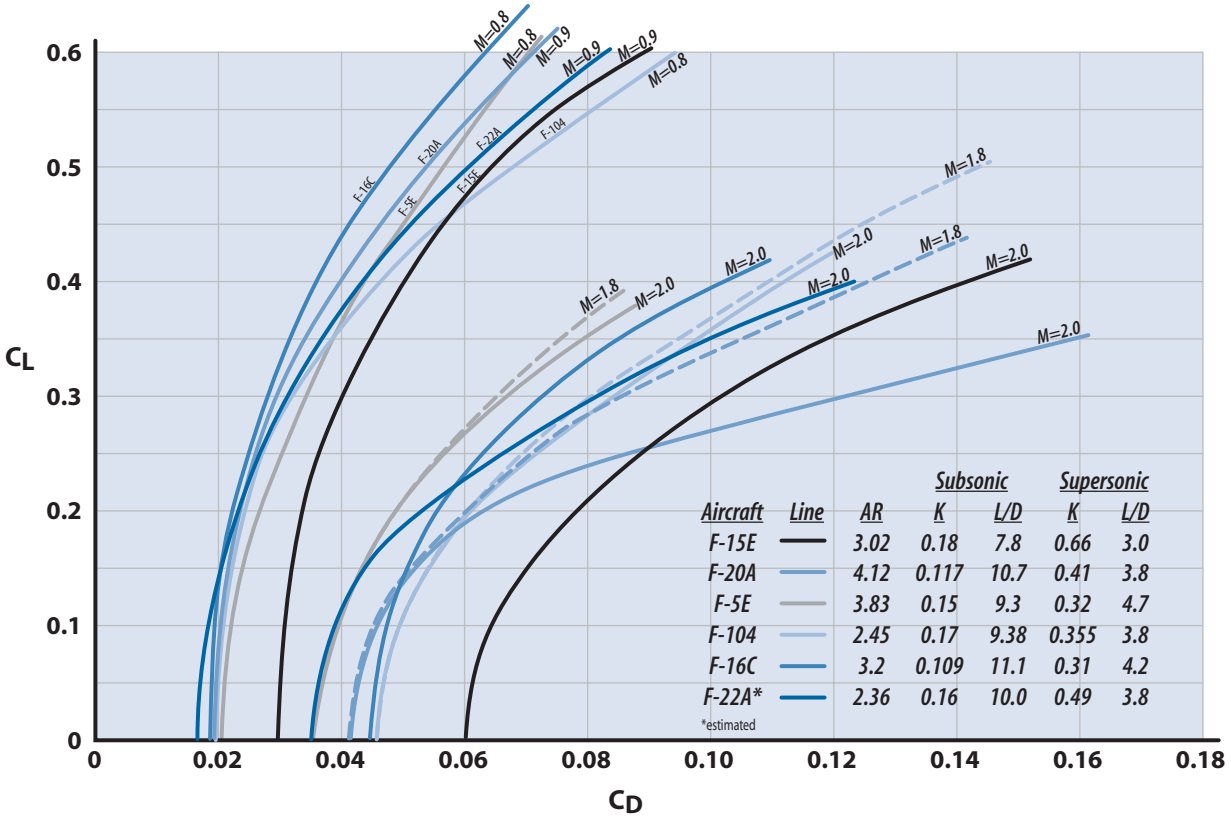

Figure G.4 Drag polars for fighter aircraft.

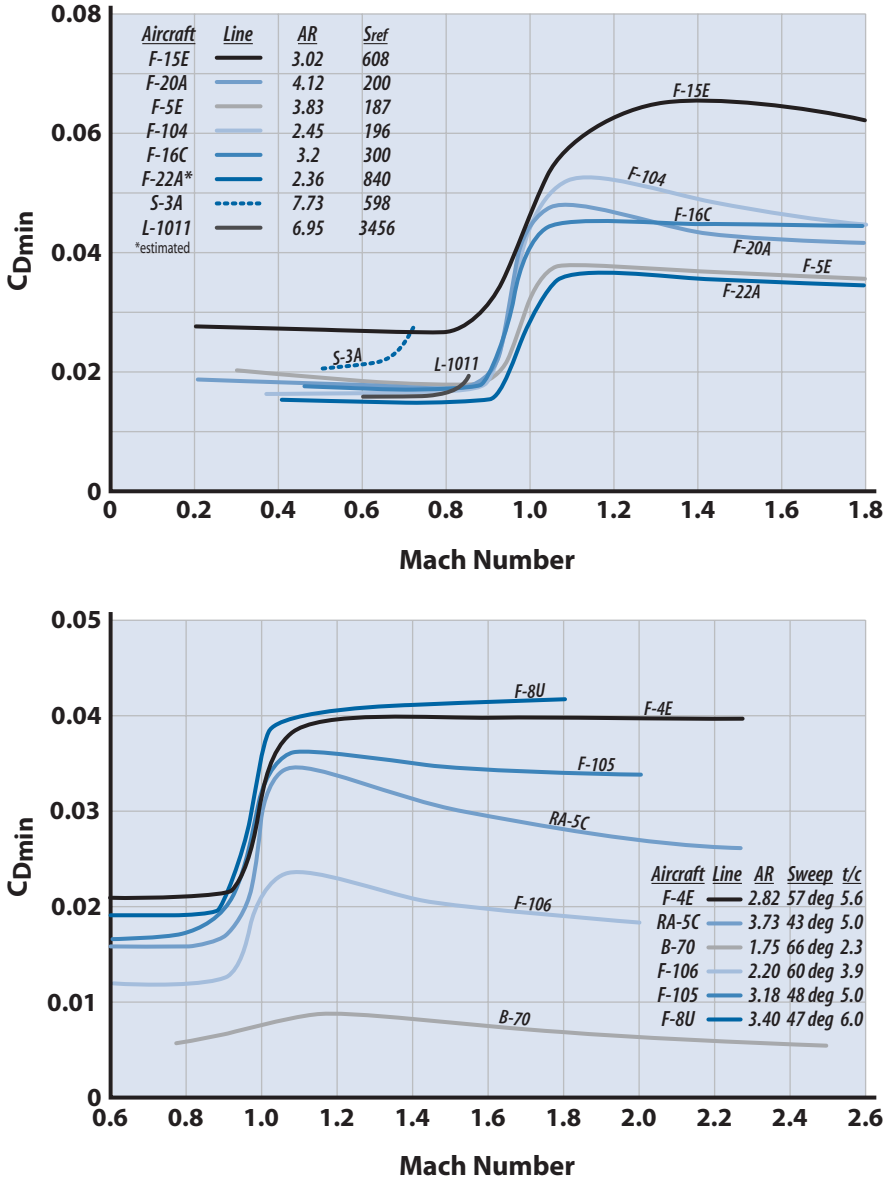

Figure G.5 $C_{D_{min}}$ vs Mach number (flight test data).

Figure G.3 shows a useful way to present aircraft aero data. Plotting L/D versus C_L shows the maximum L/D and the operating C_L region. This C_L is used to select the airfoil and to size the wing.

As discussed in Section 2.21 the subsonic C_{D_0} or $C_{D_{min}}$ is a function of the aircraft wetted area divided by the reference area. This is because the

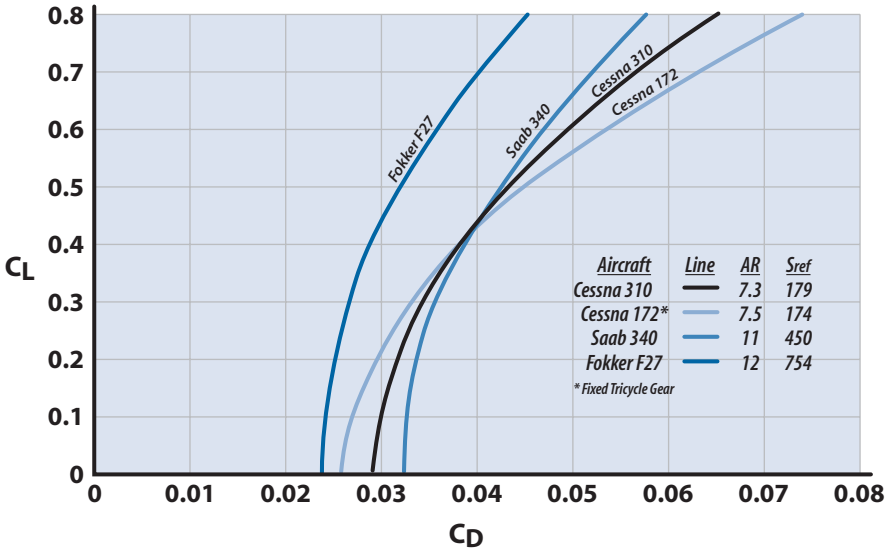

Figure G.6 Drag polars for general aviation and small transport propeller aircraft.

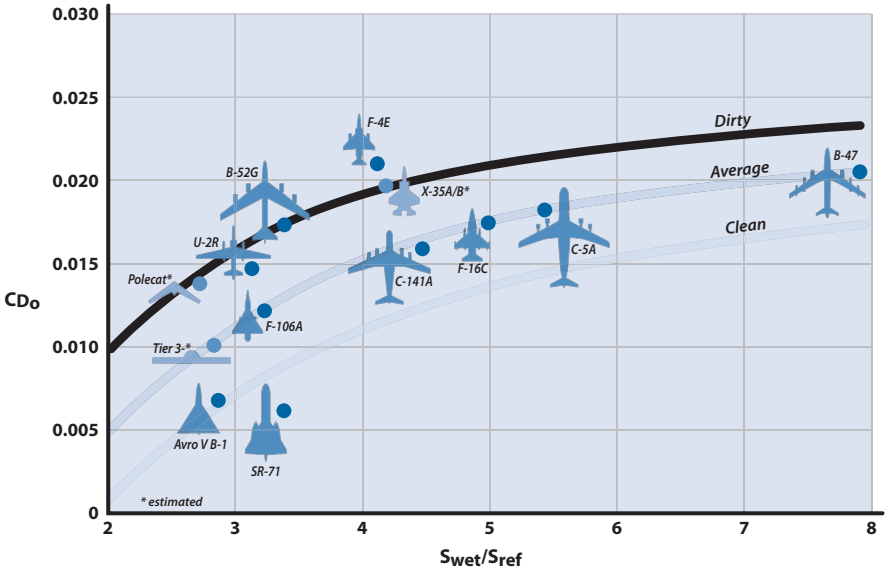

Figure G.7 Correlation of subsonic C_{D_0} with S_{wet}/S_{ref}.

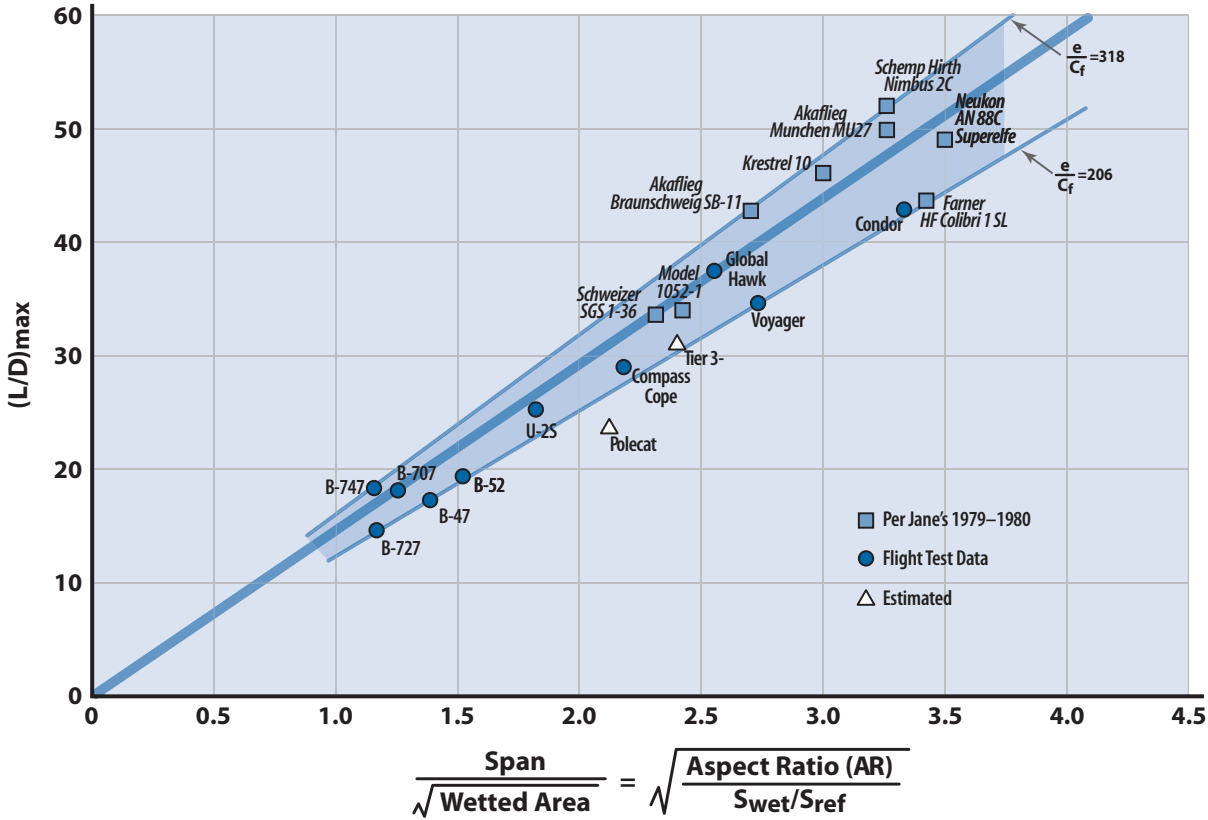

Figure G.8 Maximum lift-to-drag correlation curve.

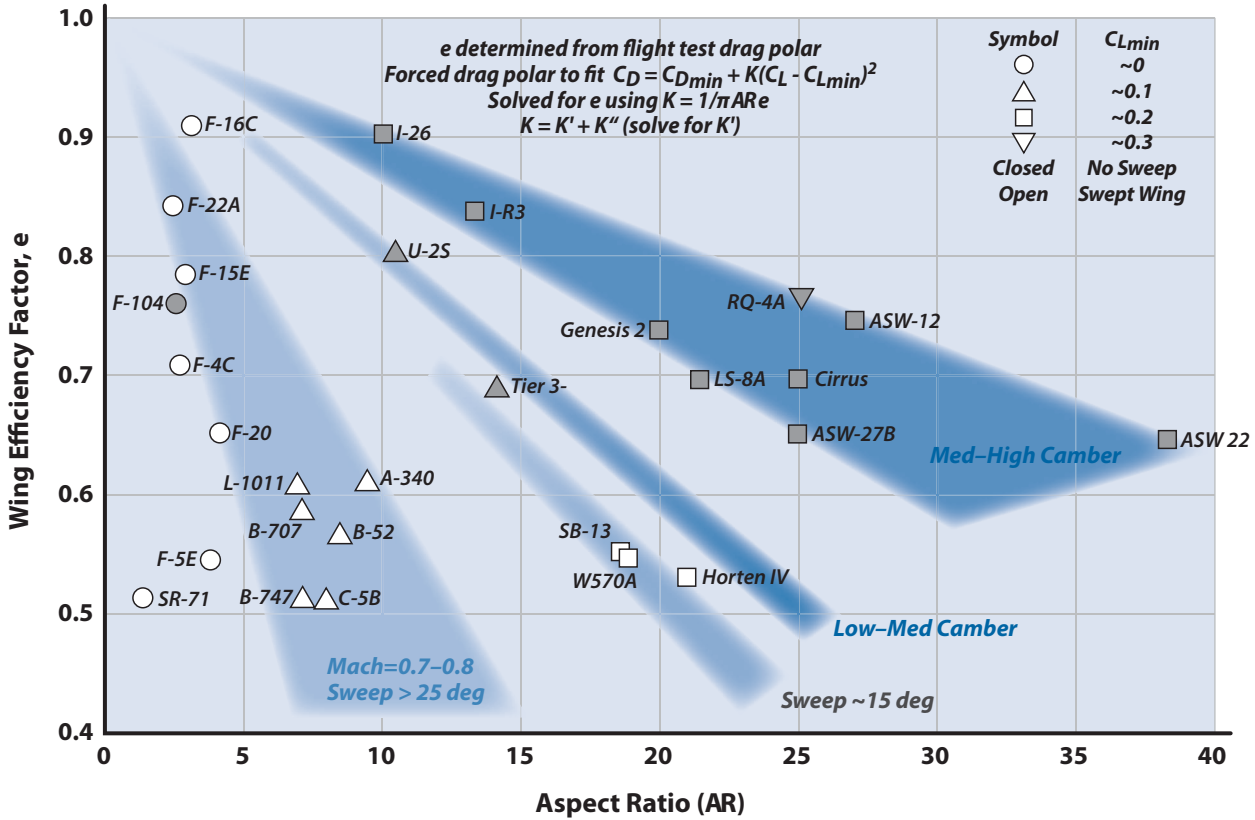

Figure G.9 Subsonic wing efficiency (*e*) vs aspect ratio for various aircraft.

subsonic C_{D_0} or $C_{D_{\min}}$ is primarily skin friction drag. This correlation is shown in Fig. G.7. The difference between the "clean" and "dirty" trend lines is primarily the excrescence/protuberance drag. The U-2R and B-52G have many external antennas. The F-4E has external weapons, targeting pods, and their associated pylons.

Figure G.8 is a very useful chart for checking the $(L/D)_{\max}$ of your design. As developed in Section 2.21 the $(L/D)_{\max} \sim (\text{span})/(S_{\text{wet}})^{1/2}$. This correlation is shown in Fig. G.8 for operational aircraft, demonstrator aircraft, and sailplanes with moderate to high aspect ratio (AR). The trend lines of e/C_f are the wing efficiency factor divided by the skin friction factor (Fig. 2.4). All aircraft need high $(L/D)_{\max}$ but it is essential for sailplanes in world-class competition. Sailplanes fall on the upper trend line because they have carefully tailored, highly efficient, high-AR wings and laminar boundary layers (operating $Re < 5 \times 10^5$). Most operational and demonstrator aircraft have good wing designs but turbulent boundary layers.

Figure G.9 is useful in obtaining a preliminary estimate of the wing inviscid factor K'. The chart is *empirical* and assumes that the aircraft drag polar can be expressed as

$$C_D = C_{D_{\min}} + K\left(C_L - C_{L_{\min}}\right)^2$$

The K in the drag-due-to-lift term is made up of the viscous drag-due-to-lift K'' (due to the viscous separation as seen in the airfoil drag polar) and the inviscid drag-due-to-lift K' (due to the influence of the trailing vortices on the wing a.c.); $K' = 1/\pi \text{AR} e'$ from finite wing theory, where e' depends on the spanwise lift distribution and is typically from 0.8 to 0.9; K'' typically ranges from 0.003 to 0.03 and is obtained from airfoil data (see Fig. 7.8 and Section F.4). The K' and K'' are combined as K. The aircraft flight test drag polar is plotted as $C_{D_{\min}}$ vs $(C_L - C_{L_{\min}})^2$. The slope K is then determined. The wing e in Fig. G.9 is determined from $K = 1/\pi \text{AR} e$.

G.2 How to Estimate Subsonic Drag Polar

Example G.1 Boeing Condor

The Condor was a high-altitude, long-endurance demonstrator aircraft built by Boeing in the 1980s for DARPA. It featured an AR = 36.6 wing with a Liebeck LD-17A airfoil, giving it an impressive maximum L/D of 42 (Fig. G.8). It had two 175-hp internal combustion engines with 16 ft diameter propellers and two stages of turbocharging. The Condor had a wing span of 200 ft, a length of 66 ft, a TOGW of 20,300 lb (empty weight of 7880 lb), and 11,080 lb of fuel. It demonstrated a flight of 58 h at 67,000 ft in 1989 and is seen in flight in the photograph (Fig. G.10).

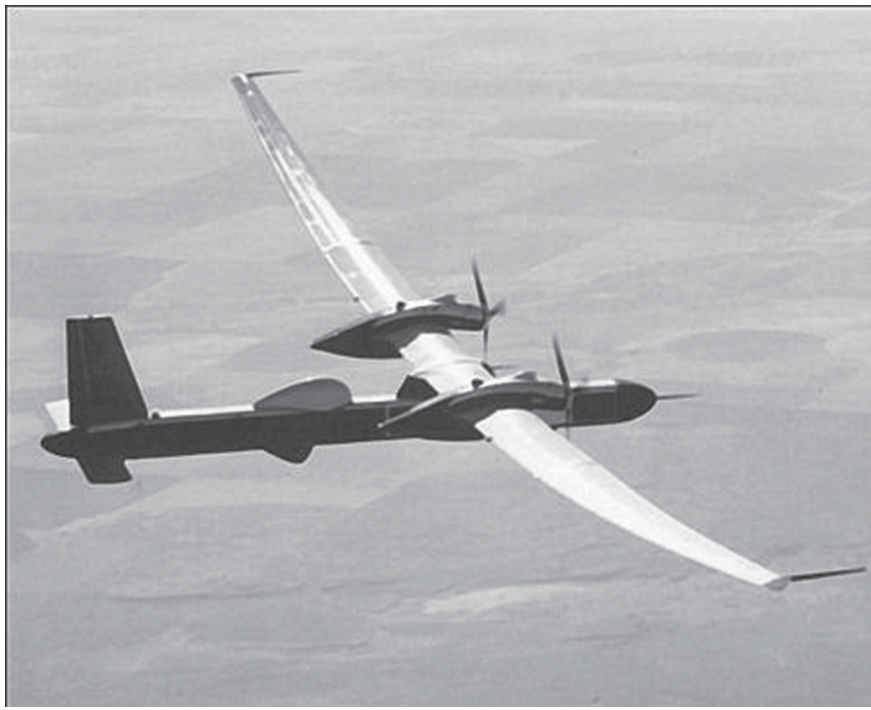

Figure G.10 Condor (courtesy of The Boeing Company).

The subsonic drag polar for the Condor operating at 60,000 ft and 200 kt will be estimated. The Reynolds number per foot is 0.3 million and the reference wing area is 1107 ft^2. The method discussed in Section 13.3 is used assuming the horizontal and vertical tails to be small wings and the engine pod to be a small fuselage. The data for determining $C_{D_{min}}$ is as follows:

Component	Wetted Area (ft^2)	Ref L (ft)	*t/c* or *l/d*	$\Delta C_{D_{min}}$
Wing	2214	6.5	0.17	0.007
Fuselage	946	66	18	0.00242
Horiz. Tail	198	4	0.10	0.00025
Vert. Tail	142	6.6	0.10	0.00046
Eng. Pods (2)	531	20.8	6.5	0.002
Total	4031			0.0123

Add 20% to account for cooling drag (from Reference 1 in Chapter 9).

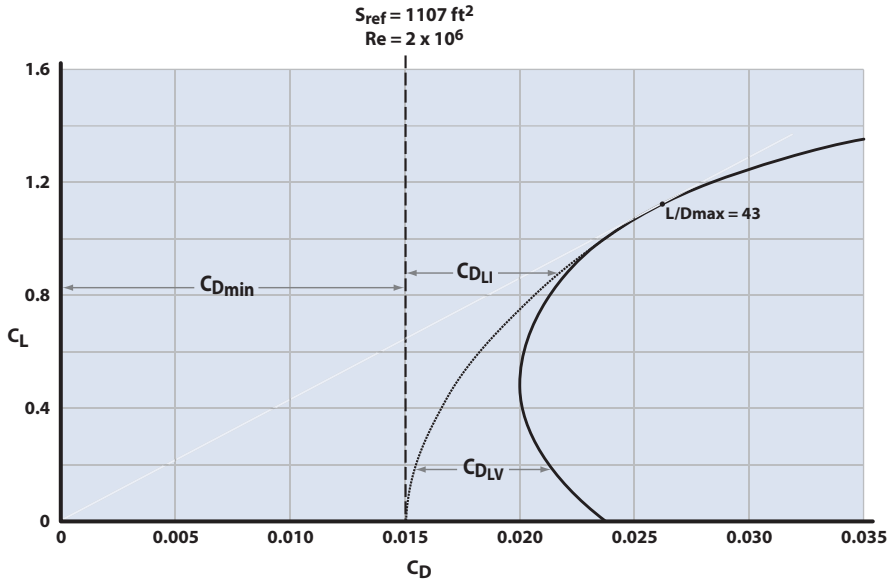

Figure G.11 Condor drag polar at 60,000 ft/200 kt.

Condor $C_{D_{min}}$	0.015
From Section F.4	$K'' = 0.006$ for $C_L < C_{l_{min}} = 1.2$
From Fig. G.9	Assume $e = 0.6$, $K = 0.0145$
Since $K = K' + K''$	$K' = 0.0085$

The expression for

$$C_D = 0.015 + 0.0085C_L^2 + 0.006\left(C_L - 1.2\right)^2 \qquad \text{(A.1)}$$

The drag polar is shown on Fig. G.11. Notice that the partition of inviscid and viscous drag-due-to-lift is quite a bit different from that shown on Fig. 2.16. This is because the LD-17A has such a large $C_{l_{min}}$. Notice also that the $C_{D_{min}}$ in equation (A-1) is very much different than the $C_{D_{min}}$ for the drag polar. This is because the $C_{D_{min}}$ buildup for Eq. (A-1) is mostly skin friction and very little pressure drag due to viscous separation. A sanity check reveals an $(L/D)_{max} = 43$, which checks with that reported for the Condor.

References

[1] Hoerner, Sighard F., *Fluid Dynamic Drag*, Midland Park, NJ, 1993.